NASA Contractor Report 4213

Structure of Wind-Shear Turbulence

G. Treviño and T. R. Laituri
Michigan Technological University
Houghton, Michigan

Prepared for
Langley Research Center
under Grant NAG1-717

National Aeronautics
and Space Administration

**Scientific and Technical
Information Division**

1989

STRUCTURE OF WIND-SHEAR TURBULENCE*§

G. Treviño† and T.R. Laituri††
Mechanical Engineering-Engineering Mechanics Dept.
Michigan Technological University
Houghton, MI 49931 USA
Tel. No. (906) 487-2551

Abstract

The statistical characteristics of wind-shear turbulence are modelled. Isotropic turbulence serves as the basis of comparison for the anisotropic turbulence which exists in a wind shear. The question of how turbulence "scales" in a wind shear is addressed from the perspective of power spectral density.

---

*Research supported by NASA-Langley Research Center, NAG 1-717.

§Presented as AIAA Paper No. 88-0581, 26th Aerospace Sciences Meeting, Reno, Nevada, January 1988.

†Associate Professor of Engineering Mechanics; Member, AIAA

††Graduate Research Assistant; Student Member, AIAA

Nomenclature

$A_{ij}(\underset{\sim}{r},t)$:	second-order anisotropic tensor
$C_{ij}(\underset{\sim}{r},t)$:	two-point time-dependent second-order velocity correlation tensor
C_k:	decay constant defined in Equ. (12)
$F_1(\bullet\bullet\bullet),F_2(\bullet\bullet\bullet)$:	polynomial basis functions for $Q(\bullet\bullet\bullet)$
$I_{ij}(\underset{\sim}{r},t)$:	second-order isotropic tensor
M_1,M_2:	mean-flow wind shear gradients
$P_m(q,r)$:	homogeneous polynomial of order m in the variables, q,r
Q(q,r,t):	third-order three-point scalar correlation function
R(r,t):	normalized scalar velocity correlation function
$S_{ijm}(\underset{\sim}{r},t)$:	third-order two-point velocity correlation tensor
U_i:	total flow velocity
$\bar{U}_i$:	mean-flow velocity
V:	airplane flight speed
a,b:	time-dependent parameters characterizing anisotropic turbulence
f(r,t)/g(r,t):	longitudinal/transverse correlation functions for isotropic turbulence
k(r,t):	scalar function peculiar to third-order velocity moments of turbulence
$\underset{\sim}{r}$:	separation vector
r:	magnitude of separation vector
u_i:	turbulent flow velocity
$w(\underset{\sim}{x},t)$:	turbulence downwash
x,z:	Cartesian coordinate variables
$\Lambda(t)$:	integral scale for isotropic turbulence

$\Delta\Lambda(t)$:	change in integral scale due to anisotropy
$\Delta(\kappa,t)$:	energy-scaling factor
α:	airplane glide-slope angle
β,γ:	dimensionless constants
κ:	non-dimensionalized wave-number
ι:	imaginary element
$\sigma(t)$:	isotropic turbulence intensity
$\Delta\sigma(t)$:	change in intensity due to anisotropy
ω:	angular frequency
θ:	dummy variable
$\phi(\kappa,t)$:	power-spectral density
$\phi^{(i)}(\kappa,t)$:	power-spectral density for isotropic turbulence
$\phi^{(a)}(\kappa,t)$:	anisotropic part of power-spectral density
τ:	time-lag
η:	generic velocity scale factor
ξ:	inverse length scale factor

1. Background

Meteorological events such as thunderstorms and unstable frontal systems have long been considered dangerous from the perspective of aviation safety. Investigations into the alarming number of recent low-level aircraft accidents involving thunderstorms around airports have revealed one meteorological culprit—a strong blast of air directed toward the ground which has come to be known as a "microburst".

The mechanism by which the microburst is created is a complex and sometimes violent one. From the investigation of a particular airliner crash at JFK airport, much was learned about the convective atmospheric dynamics which cause the microburst. It was postulated by Fujita[1] that a violent atmospheric disturbance may occur when moist upper air drops precipitation through a relatively dry air layer below it. As the precipitation evaporates, the dry layer cools; consequently, a stream of dense cold air suddenly replaces the ground-heated low-altitude air. Furthermore, as the resulting downdraft penetrates through the existing horizontal flow, turbulence is invariably generated. The downdraft eventually impacts the ground and spreads out radially. During the evolution of a microburst, the dimensions of the low-altitude phase may be on the order of 15-30 meters high with a radial spread of 2.5 kilometers. Realization of its relatively small meteorological size serves as the motivation for the term "microburst". Wind velocity information subsequently obtained from flight recorders has sustained Fujita's explanation. The typically distinguishing characteristics of the microburst are winds which are localized and variable. Abrupt changes in wind speed and/or direction over a short atmospheric distance are referred to in the literature as "wind shear". For purposes of this study, however, wind shear will be defined as a flow which has a spatially nonconstant mean-velocity

profile. Flight through a "wind shear-infected area" will tax both pilot and aircraft since related velocity gradients may drop airspeed to critically low levels. In summary, microbursts and wind shear pose an immediate threat to flight operations at low altitudes due to their adverse effects on aerodynamic lift/aircraft response.

The scenario of microburst encounter by an aircraft in the landing mode is shown in Figure 1. First the aircraft senses an uncharacteristically strong head wind. Although turbulence typically accompanies the increased airspeed, pilot confidence is high during this phase of the encounter since aircraft performance increases with the additional aerodynamic lift. Because the intent is to land the aircraft, the pilot intuitively trims. Eventually, the head wind becomes a tail wind, and at this point performance is immediately and seriously degraded since the distinct head-to-tail wind swing has reduced airspeed enough to possibly lose flying speed. In the last ten years, an estimated 575 people have been killed in commercial aircraft accidents in the United States alone due to the microburst phenomenon. Likewise, microburst-induced accidents have also been reported in Great Britain, Germany, France, Italy, Australia, and Japan. Consequently, a fundamental understanding of microbursts, related wind shear and turbulence, is a high-priority research issue.

Flight science authorities agree that the "solution" to the wind shear "problem" is multi-faceted. The existing research programs of NASA and FAA focus primarily on three elements: 1) hazard characterization; 2) sensor technology; and 3) flight management and operations. Hazard characterization is the study of the physics of the microburst phenomenon. Inherent within this phase of the research effort is analysis of aircraft aerodynamics in wind

shears and in heavy rain. Wind shear velocity profiles, rainfall effects, and turbulence models are important contributions from this component of the programs. Sensor technology deals with the prediction and detection of potentially dangerous meteorological events; it further subdivides into airport-fixed and airborne sensor technologies. Next Generation Radar fields (NEXRAD) are presently being investigated by NOAA, FAA and USAF for future use as airport radars. The other detection device is the in situ look-ahead sensor. This onboard computer system is being devised to scan the forward atmospheric environment, evaluate a "hazard index", and annunciate a warning to the pilot in a time period adequate to ensure either avoidance or escape of the threat. Look-ahead sensor technology is beyond state-of-the art, and is not expected to be operational until the mid-1990's. The third component of microburst research is flight management. Simply put, this phase concentrates on informing the pilot on how to safely get the aircraft out of a microburst encounter subject to aircraft performance constraints. An important element of such studies is flight simulation. Simulators allow pilots to experience threatening wind shears in a controlled environment, with intent to better prepare them for potential real-life events. Realistic wind shear representations in flight simulators are practical and economical, and can help crews coordinate their "escape" efforts in critical situations. Realism in the simulation of flight through hazardous atmospheric environments has improved with the introduction of lateral and vertical winds, as well as vortex and turbulence influences. The focus of the present work is in the hazard characterization aspect of the programs; its principle objectives are to model the fluid-dynamical characteristics of turbulence associated with low-level sheared mean-flow, and quantify the effect of these characteristics on aircraft response. All of these issues will be herein addressed from the perspective of power spectral density (psd).

2. Introduction

Since microbursts pose a hazardous threat to flight operations only at low altitudes, the role that the ground plays as a fixed boundary is therefore important in terms of turbulence modelling. The presence of the ground generates in the microburst a brand of turbulence which when sensed by the aircraft during its take-off or landing is both nonstationary and anisotropic. The objectives of this investigation are thus to model the statistical characteristics of same, and gain a quantitative understanding, in terms of scaling effects, of the stochastic nature of the turbulence sensed by an aircraft during a microburst encounter.

The task of mathematically describing the turbulence associated with a typical microburst (shown in Figure 1) is straightforward. The pioneering works of Taylor[2], Kármán and Howarth[3], and Robertson[4] have illustrated the well-defined fashion in which the concepts of two-point velocity correlations can be used to quantify the kinematical aspects of isotropic turbulence; Batchelor[5] extended these concepts to the case of axisymmetric turbulence—that which has a defined form of anisotropy. Axisymmetric turbulence, with its tendency to prefer one spatial direction, is the logical candidate for modelling wind shear turbulence (with its particular anisotropy resulting from the microburst impacting the ground). Although classical axisymmetric theory produces turbulence velocity correlation functions that are position-independent (homogeneous) and time-varying, the turbulence under consideration is assumed inhomogeneous and in a steady-state ("frozen") condition; nonetheless, it can be easily shown[6] that correlation functions for frozen, inhomogeneous turbulence may be converted into time-evolution equations for homogeneous turbulence by duly scaling out a characteristic velocity. Accordingly,

$C_{ij}(\underset{\sim}{x}, \underset{\sim}{r}) \sim C_{ij}(t, \underset{\sim}{r}) \to C_{ij}(\underset{\sim}{r}, t)$ and $S_{ijm}(\underset{\sim}{x}, \underset{\sim}{r}) \sim S_{ijm}(t, \underset{\sim}{r}) \to S_{ijm}(\underset{\sim}{r}, t)$, and the physics of the inhomogeneous, steady-state turbulence aligns with the physics of classical turbulence; the $(\underset{\sim}{r}, t)$-notation rather than the $(t, \underset{\sim}{r})$-notation is the accepted standard.

For the specific case of an airplane in either the take-off or landing mode, recent work[7], which incorporates axisymmetric theory, has resulted in the "airplane-sensed" two-point velocity autocorrelation for anisotropic turbulence downwash, viz.

$$C_{33}(\underset{\sim}{r}, t) = \langle w(\underset{\sim}{x}, t)\, w(\underset{\sim}{x} + \underset{\sim}{r}, t) \rangle \simeq \{\sigma^2 g\} + \{a|r| + b\} ; \qquad (1)$$

here the magnitude of $a \sim \underline{O}(\alpha)$, where α is the airplane glide-slope angle, b is a parameter (to be defined later) which can be either positive or negative, and g is the transverse correlation function of isotropic turbulence. Equation (1) is based on the assumption that during take-off or landing the aircraft senses only a small amount of anisotropy in the (necessarily) large amount present in the microburst. Note that the velocity correlation separates into isotropic and anisotropic components, and takes the general form, $C_{33}(r,t) \sim \left\{\begin{matrix}\text{isotropic} \\ \text{correlation}\end{matrix}\right\} + \left\{\begin{matrix}\text{anisotropic} \\ \text{correlation}\end{matrix}\right\}$, where

$$\left\{\begin{matrix}\text{isotropic} \\ \text{correlation}\end{matrix}\right\} = \sigma^2 g \qquad \text{and} \qquad \left\{\begin{matrix}\text{anisotropic} \\ \text{correlation}\end{matrix}\right\} = a|r| + b.$$

The contributions of isotropy and anisotropy to the total correlation are shown for $b > 0$ only in Figure 2; recall that b can be either positive or negative.

An important aspect of the ensuing analysis is how turbulence "scales" in a microburst. A common correlation used for nonstationary processes is the uniformly modulated, viz. $C(r,t) = \sigma^2(t)R(r)$ where $\sigma^2(t)$ is the time-varying modulator; implicit in this correlation is the constraint imposed on the

integral scale—that of time-invariance. In recent studies[8], however, a more general form has been formulated which incorporates time-dependence in both intensity and integral scale, viz. $C(r,t) = \eta R(\xi r)$ where $\eta = \eta(t) \equiv \sigma^2(t)$ and $\xi = \xi(t) \equiv 1/\Lambda(t)$. Allowing the correlation to evolve in such a manner permits its geometric shape to distort in time, while its r-algebraic form is retained. Figure 3 illustrates the "self-preserving" behavior of such a correlation function. With $C(0,t)$ in this case $\equiv \sigma^2(t)$, intensity for self-similarity is clearly an ordinate-axis scaling effect while the normalized correlation function, $R(\xi r)$, automatically incorporates the integral scale/abscissa-axis scaling effect. Although self-preservation is introduced here strictly from the standpoint of "scaling-effects", its hypothetical existence and subsequent analysis can be be justified on purely "dynamical system" grounds (see Appendix).

3. Power Spectral Density Analysis

The power spectral density is a common way of illustrating energy distribution versus frequency, and is an immensely popular tool in both gust analyses and turbulence simulations; mathematically, it is the Fourier transform of the autocorrelation function. The psd for the aforementioned downwash formulates as

$$\phi(\omega/V,t) = \int \langle w(x,t)w(x + r,t)\rangle e^{-i\omega r/V} dr = \int \{\sigma^2 g + a|r| + b\} e^{-i\omega r/V} dr, \quad (2)$$

where $i^2 = -1$. Since the correlation function consists of isotropic and anisotropic components, so too will its transform; specifically $\phi(\kappa,t) = \phi^{(i)}(\kappa,t) + \phi^{(a)}(\kappa,t)$, where

$$\phi^{(i)}(\kappa,t) \equiv \sigma^2 \Lambda \frac{1+3\kappa^2}{(1+\kappa^2)^2} \quad \text{and} \quad \phi^{(a)}(\kappa,t) \equiv 4\sigma^2 \Lambda \left\{\frac{\Delta\Lambda}{\Lambda}\right\} \frac{1-\cos(\kappa b/a\Lambda)}{(\kappa b/a\Lambda)^2}. \quad (3)$$

Here $\phi(\kappa,t)$ is the total psd sensed by the aircraft as it flies through the

microburst, $\kappa \equiv \omega\Lambda/V$ a non-dimensionalized wave number, σ the isotropic intensity, Λ the longitudinal correlation length (integral scale), and $\Delta\Lambda$ the change in integral scale due to anisotropy. The scaling effects discussed earlier are evident upon inspection of Equ. (3).

The distinct advantage that the psd representation has over its transform partner, the autocorrelation function, is its more defined statement of the modelling parameters of anisotropy, viz. $\Delta\Lambda$, a, and b, in relation to total turbulent energy. For a glide-slope which is maintained during a microburst encounter, it follows that a $\simeq$ constant since (recall) magnitude $\{a(t)\} \sim \underline{Q}(\alpha)$. Hence, b plays the more important role in terms of modelling the anisotropy due to the boundary presence. Since b is related to intensity by $\sigma^2 + b = (\sigma + \Delta\sigma)^2$, $\Delta\sigma \sim$ increment in intensity contributed by anisotropy, for neglected higher-order terms b becomes

$$b = \sigma^2 \left\{\frac{2\Delta\sigma}{\sigma} + \left[\frac{\Delta\sigma}{\sigma}\right]\right\} \simeq 2\sigma^2\left[\frac{\Delta\sigma}{\sigma}\right] = 2\sigma\Delta\sigma; \qquad (4)$$

note that for pure isotropic turbulence, $b \equiv 0$. One way to quantify the collective effects of $\Delta\Lambda$, a, and b on the airplane-sensed turbulence is to introduce an "energy scaling factor", defined as $\Delta(\kappa,t) = \phi^{(a)}(\kappa,t)/\phi^{(i)}(\kappa,t)$. To analyze the effect of $\Delta\Lambda/\Lambda$ on $\Delta(\kappa,t)$, set $b/(a\Lambda) \simeq$ constant; typical values of $\sigma = 5$ ft/s, $\Lambda = 1000$ ft, $V = 225$ ft/s and $a \sim \underline{Q}(\alpha) = \underline{Q}(3^{\circ}) = \underline{Q}(0.052$ rad) are chosen, and $\Delta\sigma/\sigma$ is allowed to vary up to 0.5 (a feasible value for wind-shear turbulence severity). Incorporating Equ. (4) gives $b/(a\Lambda) \simeq \underline{Q}(0.5)$. Figure 4 shows that for $\Delta\Lambda/\Lambda = 0.1$, the energy scaling factor is as high as 35% for $0 \leq \kappa \leq 2$ ($0 \leq \omega \leq 0.45$ rad/sec)—a frequency range which falls within that specified for the guidance and control phases of an aircraft mission involving a wind shear. Hence, a realistic estimate of the energy transferred to the airplane requires that anisotropy be accounted for in both turbulence models and related flight simulations.

4. Constraints Imposed by Navier-Stokes

Knowledge of the sheared mean-wind/turbulence interplay requires that the governing equation of the fluid be considered. The Navier-Stokes equation for a turbulent, high Reynolds number, steady-state fluid with both body and pressure forces neglected is

$$\frac{\partial(U_i U_m)}{\partial x_m} \simeq 0. \tag{5}$$

With $U_i = U_i + u_i$, the two-point correlation method[9] yields

$$\frac{\partial}{\partial t} C_{ij} + \frac{\partial U_i}{\partial x_m} C_{mj} - 2 \frac{\partial}{\partial r_m} S_{imj} + \frac{\partial U_j'}{\partial x_m'} C_{im} = 0 \tag{6}$$

where $C_{ij} \sim C_{ij}(\underset{\sim}{r},t) = \langle u_i u_j' \rangle$, $S_{imj} \sim S_{imj}(\underset{\sim}{r},t) = \langle u_i u_m u_j' \rangle$ and (cf. Figure 1) $\underset{\sim}{r} = (r, 0, \alpha r)$; index contraction results in

$$\frac{\partial}{\partial t} C_{ii} + \frac{\partial U_i}{\partial x_m} C_{mi} + \frac{\partial U_i'}{\partial x_m'} C_{im} - 2 \frac{\partial}{\partial r_m} S_{imi} = 0. \tag{7}$$

Equation (7) requires the solution of separate isotropic and anisotropic dynamical problems, viz.

$$\frac{\partial}{\partial t} I_{ii} - 2 \frac{\partial}{\partial r_m} S_{imi} = 0 \tag{8}$$

and

$$\frac{\partial}{\partial t} A_{ii} + \frac{\partial U_i}{\partial x_m} C_{mi} + \frac{\partial U_i'}{\partial x_m'} C_{mi} = 0 , \tag{9}$$

where [7,10] $I_{ij} + A_{ij} = C_{ij}$. The basis for a scaling comparison (the isotropic case) will be considered first.

Introducing the f and g functional representations for the correlation tensors gives a result whose first integral is the Kármán-Howarth equation for high Reynolds number isotropic turbulence[9], viz.

$$\frac{\partial}{\partial t} (\sigma^2 f) - \sigma^3 \left[\frac{4k}{r} + \frac{\partial k}{\partial r} \right] \simeq 0, \tag{10}$$

where $k = k(r,t)$ is the scalar function required to specify third-order

velocity product moments. Since turbulence self-interaction is not altered by self-preservation, it follows that k(r,t) also has such an evolution with time, i.e. $k(r,t) \simeq k(\xi r) = k(r/\Lambda)$. Incorporation of this feature into the r-integration of the Kármán-Howarth equation results in

$$\frac{d}{dt}\{\sigma^2(t)\Lambda(t)\} = \sigma^3 C_k, \tag{11}$$

where

$$C_k \equiv \int_0^\infty \left\{\frac{4k(\theta)}{\theta} + \frac{\partial k(\theta)}{\partial \theta}\right\} d\theta = \text{negative scale-independent constant}, \tag{12}$$

and $\theta = r/\Lambda$; a specific numerical value of C_k will be determined later. Solution of Equ. (11) gives the time-dependence,

$$\Lambda(t) = \frac{C_k}{\sigma^2(t)} \int \sigma^3(t)dt, \tag{13}$$

for the integral scale. The power-law form for isotropic intensity, $\sigma^2(t) \sim t^n$, $n = \pm 1, +2, \ldots$, converts Equ. (13) into

$$\Lambda(t) \sim \frac{2C_k}{3n+2} t^{(n+2)/2}, \quad N = \pm 1, \pm 2, \ldots; \tag{14}$$

for $n = -1$, $\Lambda(t) \sim \underline{O}(t^{1/2})$.

To consider the anisotropic part of the problem, viz. Equ. (9), gradients must first be defined. The two wind-shear profiles chosen for analysis are illustrated in Figures 5 and 6, and will hereinafter be referred to as "Shear Flow I" and "Shear Flow II", respectively. Note that both profiles have a "head-to-tail wind swing", a phenomenon frequently observed in microburst encounters. The mean velocity for Shear-Flow I is $U_i = \{U(z),0,0\} \equiv \{M_1 z,0,0\}$ as shown in Figure 5; M_1 is negative on the headwind side of the microburst and positive on the tailwind side. Analysis of Shear Flow II is restricted to the two-dimensional case with $U_i = \{U(x),0,W(z)\}$ and gradients of the form $\frac{dU}{dx} = -\frac{dW}{dz} = M_2 > 0$. Incorporation of Shear-Flow I characteristics into

Equ. (9) yields

$$\frac{\partial}{\partial t}\,(a|r|+b) - M_1\sigma^2\alpha r\,\frac{\partial f}{\partial r} + M_1\alpha r\sigma^2\,\frac{\partial(f+2g)}{\partial r} \simeq 0\ ; \tag{15}$$

integration in r from 0 to ∞ produces

$$\frac{d}{dt}\,\{\sigma^2(t)\Delta\Lambda(t)\} - M_1\sigma^2(t)\alpha\Lambda(t) = 0\ , \tag{16}$$

where $\int_0^\infty (a|r| + b)\,dr \equiv \sigma^2\Delta\Lambda(t)$. The solution to Equ. (16) is

$$\Delta\Lambda(t) = \frac{M_1\alpha}{\sigma^2(t)} \int \sigma^2(t)\Lambda(t)dt. \tag{17}$$

For $\sigma^2(t) \sim t^n$ and the integral scale of Equ. (14), Equ. (17) becomes

$$\Delta\Lambda(t) \sim \frac{4M_1C_k\alpha}{(3n+2)(3n+4)}\,t^{(n+4)/2},\ n = \pm1,\ \pm2,\ \ldots; \tag{18}$$

specifically, $\Delta\Lambda(t) \sim \underline{O}(t^{3/2})$ for $\sigma^2(t) \sim t^{-1}$. A similar analysis for Shear-Flow II yields

$$\Delta\Lambda(t) \sim -\frac{4M_2C_k}{(3n+2)(3n+4)}\,t^{(n+4)/2},\ n = \pm1,\ \pm2,\ \ldots$$

Like Shear Flow I, Shear Flow II has $\Delta\Lambda(t) \sim \underline{O}(t^{3/2})$ for $\sigma^2(t) \sim t^{-1}$.

5. Determination of C_k

The theory of turbulence strictly prohibits the presence in the analysis of any adjustable constants; therefore a full closure of the dynamical equation is not achieved until a value for C_k is determined. The fact that C_k is formed from an integral of k(•••) (cf. Equ. (12)) explicitly suggests that aside from some fundamental limiting constraints, viz. $\lim_{r\to\infty}\{k(\bullet\bullet\bullet)\} \sim \underline{O}(r^3)$ and $\lim_{r\to 0}\{k(\bullet\bullet\bullet)\} = 0$, the exact functional form of k(•••) is not critical, i.e. k(•••) itself is not necessarily a unique function. All that is required for any and all possible k(•••), say $k(\bullet\bullet\bullet) \to k_N(\bullet\bullet\bullet)$, N = 1,2,3, . . ., is that $\{4\int_0^\infty r^{-1}k_N(r,t)dr\} = C_k$ be independent of N. A preliminary step is therefore to develop a representative algebraic form for $k(r,t) \sim k(r/\Lambda)$.

To accomplish this while simultaneously saying as little as possible about $k(\bullet\bullet\bullet)$ itself, it is here proposed to kinematically describe the three-point correlation, $<u(x,t)u(x+q,t)u(x+r,t)> = Q(q,r,t)$, where $u(x,t)$ is only one component of the three-component turbulence velocity field and x is a one-dimensional position vector, i.e. $\underset{\sim}{x} = (x,0,0)$, etc. Note that for self-preservation, this correlation accordingly scales as $Q(q,r,t) = \sigma^3(t)s(q/\Lambda,r/\Lambda)$, where $s(0,r/\Lambda) \equiv k(r/\Lambda)$; furthermore, the functional form of $Q(\bullet\bullet\bullet)$ is such that it must satisfy certain symmetry properties, viz. $Q(q,r,t) = Q(r,q,t) = Q(-q,r-q,t)$[11]. Since $Q(\bullet\bullet\bullet)$ expanded in a Taylor's series about $q = r = 0$ produces

$$Q(q,r,t) \simeq a_0 + a_1 q + b_1 r + a_2 q^2 + c_2 qr + b_2 r^2 + \ldots ,$$

it follows from the required symmetry that the time-dependent parameters, a_m, b_m, and c_m, $m = 0,1,2,\ldots$, cannot be completely arbitrary. In fact they must each be such that eventually $Q(\bullet\bullet\bullet)$ expresses as[12]

$$Q(q,r,t) = \sum_{m=0}^{\infty} A_m(t)P_m(q,r)$$

where each $P_m(\bullet\bullet\bullet)$ is a homogeneous polynomial in q, r and individually must themselves satisfy the same symmetry as $Q(q,r,t)$, i.e. $P_m(q,r) = P_m(r,q) = P_m(-q,r-q)$, $m = 0,1,2,\ldots$. Fortunately, there are only two (2) fundamental such forms, viz. $F_1(q,r) = q^2 - qr + r^2$ and $F_2(q,r) = 2q^3 - 3q^2r - 3qr^2 + 2r^3$, since any other higher-order such form can be represented as a combination of $F_1(\bullet\bullet\bullet)$ and/or $F_2(\bullet\bullet\bullet)$; there is no <u>linear</u> homogeneous algebraic form in q,r which satisfies the required symmetry. For example, the fourth-order polynomial is identical to $\{F_1(q,r)\}^2$, while the fifth-order one is identical to $\{F_1(q,r)F_2(q,r)\}$. The existence of such a complete set of polynomial basis functions for <u>any</u> sequence of systematically generated algebraic forms was originally established in a theorem formulated by David Hilbert in 1890[13]. The theorem need not be quoted here, but the essence of it is that if an infinite sequence of algebraic forms (the sequence here is $P_0(q,r) = 1$,

$P_1(q,r) \equiv 0$, $P_2(q,r) = q^2 - qr + r^2$, $P_3(q,r) = 2q^3 - 3q^2r - 3qr^2 + 2r^3$, etc.) is constructed according to some general rule (the "rule" here is the required q,r-symmetry), there comes a point in the construction where the set of all available independent such forms is exhausted and any form constructed thereinafter contains absolutely no new information, being merely a modification/repetition of what has already preceded. What this means for the case at hand is that the most general sixth-order form must be a linear combination of the products, $F_1^3(q,r)$ and $F_2^2(q,r)$, while a seventh-order such form is $\{F_1^2(q,r)F_2(q,r)\}$. A simple appropriate algebraic expression for $Q(q,r,t)$ which for $q \equiv 0$ fits data reported by Stewart[14] is thus

$$Q(q,r,t) \simeq \sigma^3(t) \frac{AF_2(q,r)}{\{1 + BF_1(q,r)\}^2},$$

where $A = \beta\Lambda^{-3}(t)$, $B = \gamma\Lambda^{-2}(t)$, and $\beta,\gamma \sim$ dimensionless constants; accordingly,

$$k(r,t) \sim k(r/\Lambda) \simeq \frac{2\beta(r/\Lambda)^3}{\{1 + \gamma(r/\Lambda)^2\}^2}.$$

The specific β and γ for the data sets highlighted by Stewart (loc. cit.) are:

Curve 1 (cf. Figure 7); $\beta = -1.48$, $\gamma = 7$; Re = 5300;

Curve 2 (cf. Figure 8); $\beta = -3.0$, $\gamma = 12$; Re = 21,200;

Curve 3 (cf. Figure 9); $\beta = -7.42$, $\gamma = 22$; Re = 42,400;

The value of C_k which most closely approximates all three cases is $C_k \simeq -0.16\pi$.

6. Conclusions and Concluding Remarks

Since integral scale provides a measure of turbulence randomness[7,10], realistic estimates of this scale are essential to ensure related flight simulation fidelity. The role played by anisotropy in a wind shear encounter is quantified in the correlation length, $L \equiv \Lambda(t) + \Delta\Lambda(t)$. As an aircraft in the landing mode penetrates the headwind portion of Shear Flow I, $\Delta\Lambda > 0$

since M and α are negative in this phase of flight. The turbulence sensed there by the aircraft is therefore less random than that predicted by isotropic theory. The tailwind phase of such an encounter provides $\Delta\Lambda < 0$—a more random turbulence in comparison with isotropy. A similar landing mode analysis of Shear-Flow II yields negative $\Delta\Lambda$ on both sides of the microburst, thus making the attendant turbulence more random than the isotropic case in all phases of the encounter.

The significance of anisotropy in microburst turbulence models has herein been considered from the perspective of self-similarity in the turbulence power spectral density. The considered energy scaling factor clearly defines the inadequacy of using isotropic theory only to estimate the necessarily anisotropic turbulent energy in a typical wind shear. The formulated psd representation of the turbulent downwash is a major step towards enhanced simulation of low-level turbulence, with the relative importance of the characteristics considered above becoming fully quantified only upon eventual flight-simulator implementation.

Acknowledgements

This research was supported by the NASA-Langley Research Center through the ASEE and LARSS programs. The authors wish to thank Drs. R.L. Bowles and B.T. McKissick (both of NASA-LaRC) and Mr. D. Staublin and Mr. A. Rosenberger (both of Michigan Technological University) for their collective participation in this work.

References

[1]Fujita, T.T., "Spearhead Echo and Downburst Near the Approach End of a John F. Kennedy Airport", Satellite and Mesometeorological Research Project, SMRP Research Paper 137, 51 pp., 1976.

[2]Taylor, G.I., "Statistical Theory of Turbulence," Proceedings of the Royal Society, A, Vol. 151, 1935, pp. 412-478.

[3]von Kármán, T. and Howarth, L., "On the Statistical Theory of Isotropic Turbulence," Proceedings of the Royal Society, A, Vol. 164, 1937, pp. 192-215.

[4]Robertson, H.P., "Invariant Theory of Isotropic Turbulence," Proceedings of the Cambridge Philosophical Society, Vol. 36, 1940, pp. 209-233.

[5]Batchelor, G.K., "Theory of Axisymmetric Turbulence," Proceedings of the Royal Society, A, Vol. 186, 1946, pp. 480-502.

[6]Treviño, G., "Turbulence for Flight Simulation," Journal of Aircraft, Vol. 23, April 1986, pp. 348-349.

[7]Treviño, G., "Airplane Flight Through Wind-Shear Turbulence," Journal of Aircraft, Vol. 23, Sept. 1986, pp. 733-735.

[8]Treviño, G., "Time-Invariant Structure of Nonstationary Atmospheric Turbulence," Journal of Aircraft, Vol. 22, Sept. 1985, pp. 827-828.

[9]Batchelor, G.K., Theory of Homogeneous Turbulence, Cambridge University Press, Cambridge, U.K., 1967.

[10]Treviño, G., "Turbulence Structure in Microburst Phenomena," Journal of Aircraft, Vol. 24, April 1987, pp. 283-285.

[11]Proudman, I. and Reid, W.H., "On the Decay of a Normally Distributed and Homogeneous Turbulent Velocity Field," Philosophical Transactions of the Royal Society of London, Vol. 247.A.926, 1954, pp. 163-189.

[12]Treviño, G., "Invariant Structure in Nonstationary Behavior", forthcoming in Journal of Sound and Vibration.

[13]Hilbert, D., "Über die Theorie der Algebraischen Formen," Mathematische Annalen, Vol. 36, 1890, pp. 473-534.

[14]Stewart, R.W., "Triple Velocity Correlations in Isotropic Turbulence," Proceedings of the Cambridge Philosophical Society, Vol. 47, 1951, pp. 146-157.

Appendix: The Case for Self-Preservation

Nonstationary behavior whose time-evolution can be effected by two time-dependent scaling effects is important not only because of its relatively simple features, but also because of its immediate practical application. For nonstationary processes the two-time correlation function, $Q(t_1,t_2) = \langle w(t_1)w(t_2)\rangle$, can be considered as a two degree-of-freedom system in which $t = (t_1 + t_2)/2$ and $\tau = t_2 - t_1$ play the role of uncoupled principal coordinates; indeed in the (t,τ)-coordinate reference frame the two degree-of-freedom system at hand is instead duly converted into one whose physical characteristics accordingly vary with time, i.e. $Q(t_1,t_2) \rightarrow Q(t,\tau) \rightarrow C(t,r/V) \sim C(t,r)$, where $V \simeq r\tau$. And even though time-varying systems can be regarded as filters which "select" eigenfunctions in the pure sense rather than just simple sinusoids, the natural tendency in their analysis is to treat them as systems whose properties do not change "appreciably" with repect to time. The underlying motivation for this approach is that classical modal analysis is not explicitly restricted to systems which are time-invariant only; it is only necessary that the differential equation governing the system, as well as the boundary conditions, be separable into a function of time alone and in this case a function of non-dimensionalized length alone, i.e. that temporal changes in the system be in some sense "uniform". The suggested separation for dynamical systems is thus the essence of self-preservation for nonstationary behavior in random processes. The mathematics of same proceeds as follows. Consider the most general case of time-varying intensity and integral scale, viz. $C(t,\tau)=\sigma(t-\tau/2)\sigma(t+\tau/2)R(t,\tau)$, $\tau = r/V$. If $\sigma(\bullet\bullet\bullet)$ is expanded in Taylor's series about $\tau = 0$, the result for $C(t,\tau)$ is

$$C(t,\tau) \simeq \sigma^2(t)\{1 - \tau^2/4T^2\}R(t,\tau)$$

where only linear terms in τ have been retained for $\sigma(t \pm \tau/2)$, and $T =$

$\sigma(t)\left[\frac{d\sigma}{d\tau}\right]^{-1}_{\tau=0}$ is the time-dependent scale over which $\sigma(t)$ may be assumed to vary linearly with τ, viz.

$$\sigma(t \pm \tau/2) \simeq \sigma(t)\{1 \pm \tau/2T\}.$$

Since R(•••) scales with $\Lambda(t)$, i.e. $R(t,\tau) \sim R(\tau/\Lambda)$[†], and $\sigma(•••)$ scales with T, the modified expression,

$$C(t,\tau) \simeq \sigma^2(t)\{1 - (\tau/2\Lambda)^2(\Lambda/T)^2\}R(•••) ,$$

allows for analysis of the coupling between the two scales, T and Λ. Note that as far as R(•••) is concerned, R(•••) $\simeq$ 0 for $\tau > \Lambda$, so that the major contribution to $C(t,\tau)$ from R(•••) itself is from values of $\tau < \Lambda$. Therefore, if $T \gg \Lambda$, it follows that $C(t,\tau) \simeq \sigma^2(t)R(•••)$, i.e. the τ-dependence of $C(t,\tau)$ is determined by R(•••) only and is unaffected by the τ-dependence of $\{\sigma(t - \tau/2)\sigma(t + \tau/2)\}$.

[†] $\Lambda \sim \Lambda(t)$ in this expression considered as a "time-length" scale.

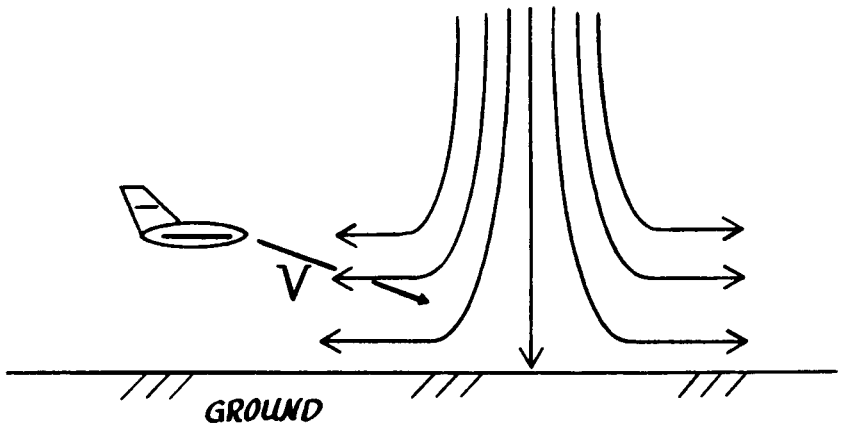

Figure 1: Schematic of a typical microburst encounter by an aircraft attempting to land.

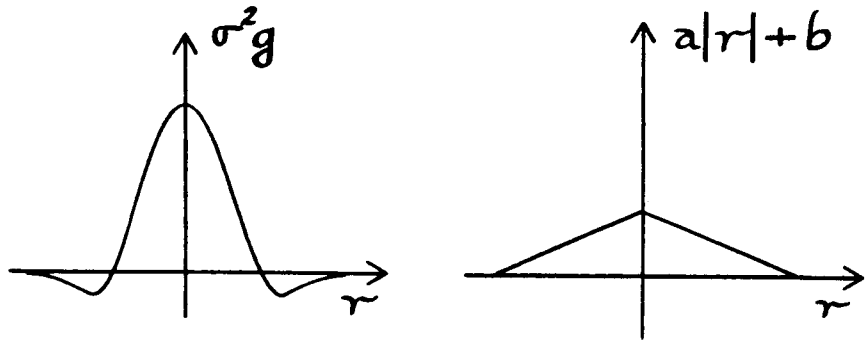

Figure 2: Contributions of isotropy and anisotropy to the downwash correlation.

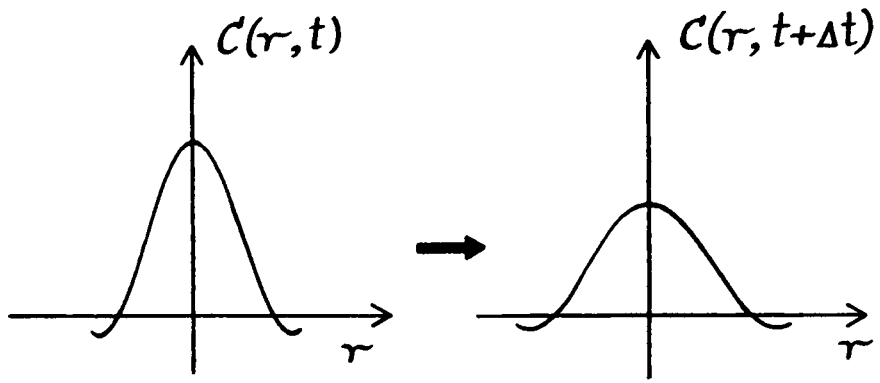

Figure 3: Time-evolution of a self-similar or self-preserving correlation function; note the explicit two scaling-effects features.

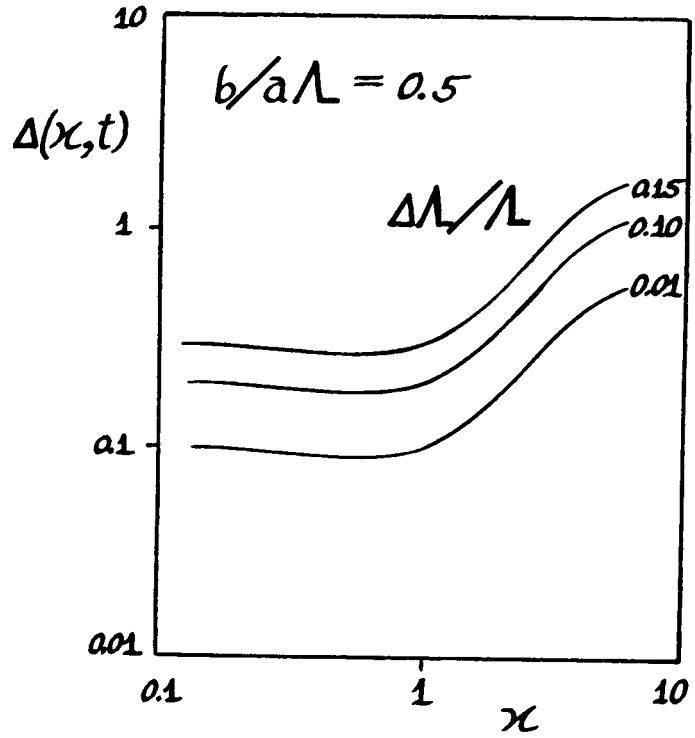

Figure 4: Energy scaling factor quantifying the effects of anisotropy, i.e. $\Delta\Lambda/\Lambda$.

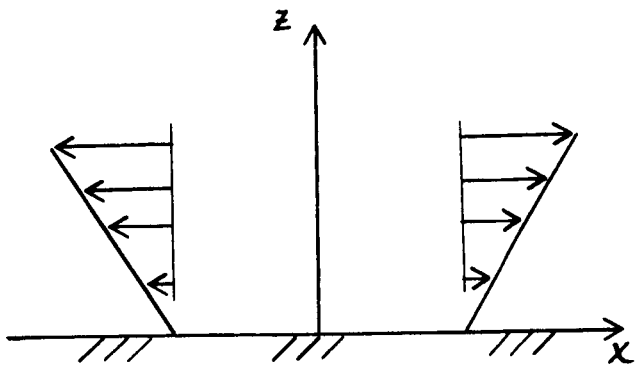

Figure 5: Sheared microburst mean wind consistent with "no-slip" condition.

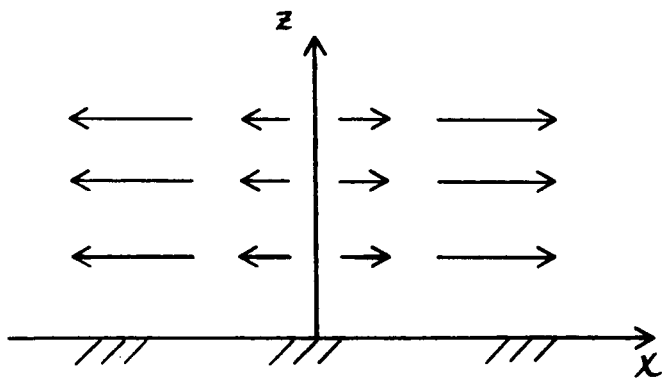

Figure 6: Sheared microburst mean wind for continuously varying headwind/tailwind.

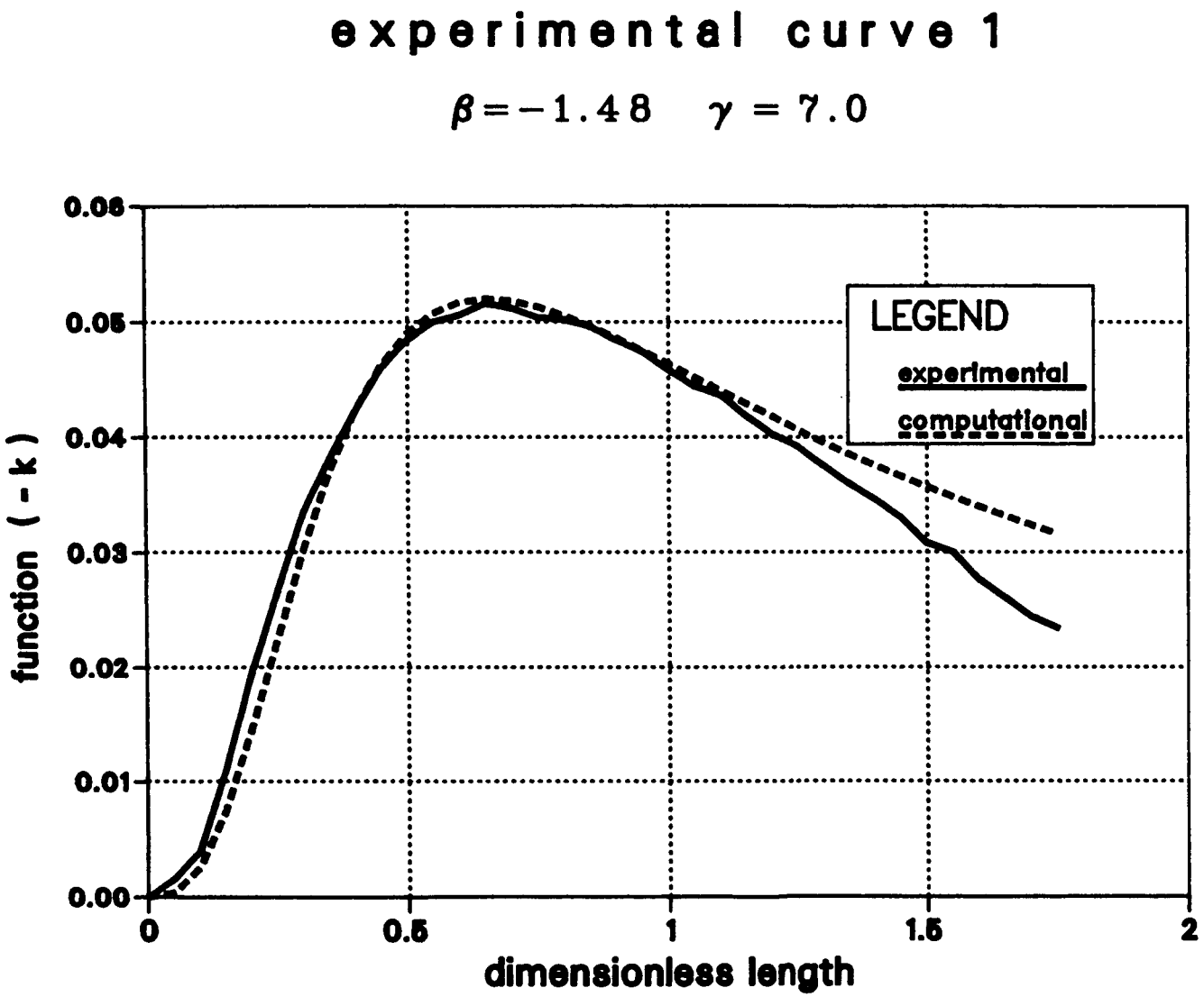

Figure 7: Triple-velocity curve, k(. . .), obtained by Stewart; broken line is theoretical curve.

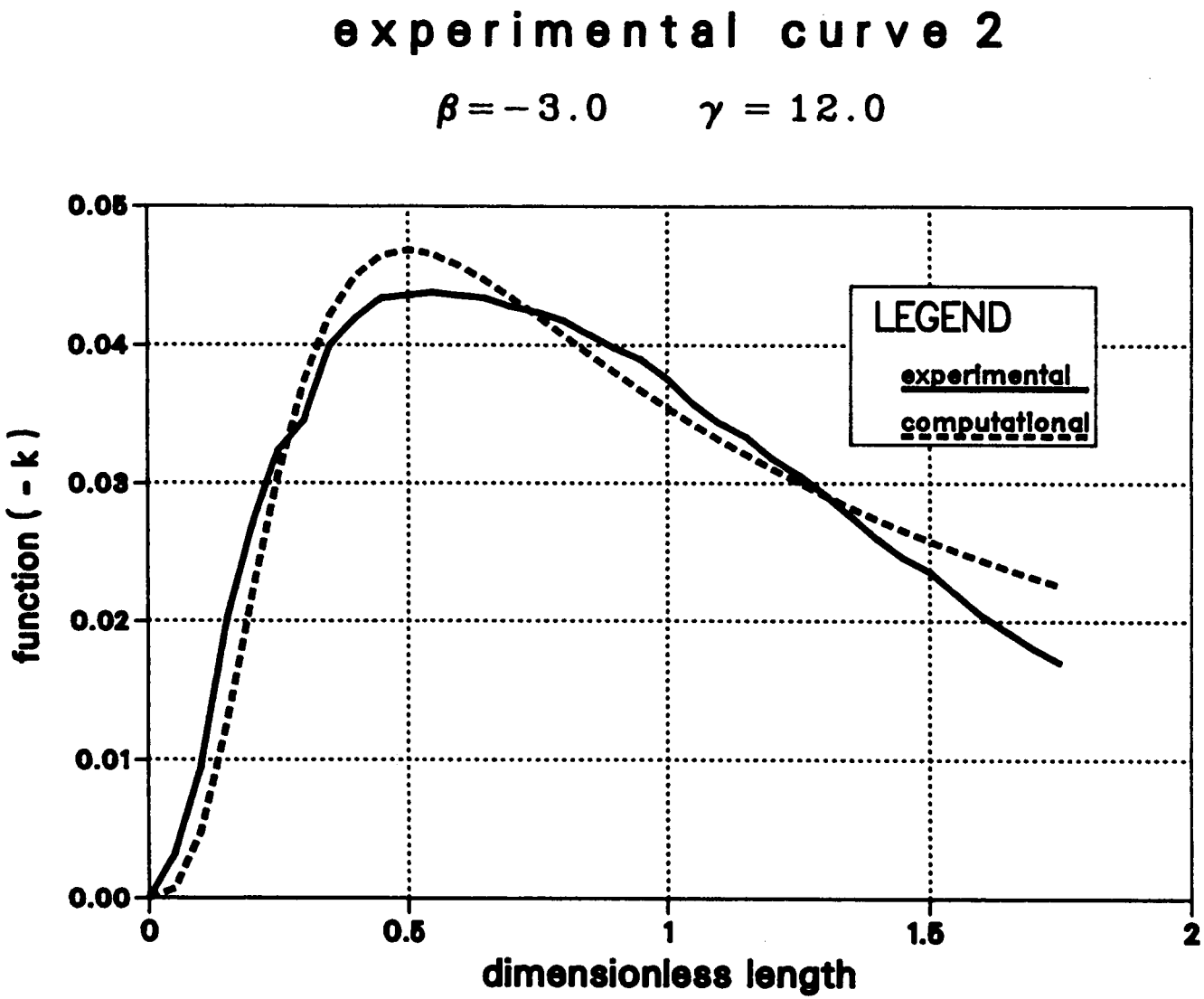

Figure 8: Triple-velocity curve, k(. . .), obtained by Stewart; broken line is theoretical curve.

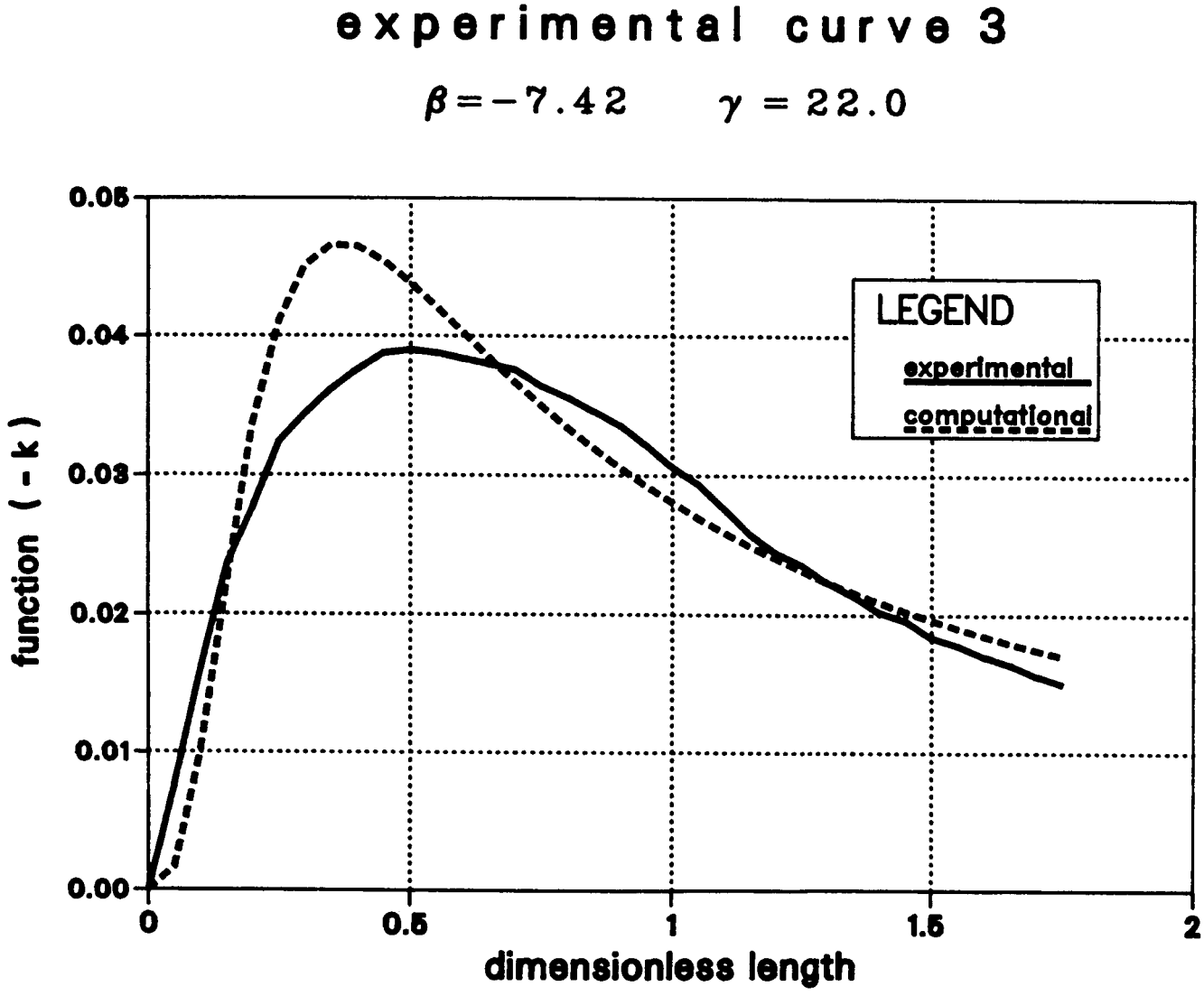

Figure 9: Triple-velocity curve, k(. . .), obtained by Stewart; broken line is theoretical curve.

NASA
National Aeronautics and Space Administration

Report Documentation Page

1. Report No.	2. Government Accession No.	3. Recipient's Catalog No.
NASA CR-4213		

4. Title and Subtitle	5. Report Date
Structure of Wind-Shear Turbulence	January 1989
	6. Performing Organization Code

7. Author(s)	8. Performing Organization Report No.
G. Treviño and T. R. Laituri	
	10. Work Unit No. 505-67-41

9. Performing Organization Name and Address	11. Contract or Grant No.
Mechanical Engineering-Engineering Mechanics Dept. Michigan Techological University Houghton, MI 49931	NAG1-717
	13. Type of Report and Period Covered
12. Sponsoring Agency Name and Address	Contractor Report
National Aeronautics and Space Administration Langley Research Center Hampton, VA 23665-5225	14. Sponsoring Agency Code

15. Supplementary Notes
Langley Technical Monitor: Burnell T. McKissick
Final Report

Also presented as AIAA Paper No. 88-0581, 26th Aerospace Sciences Meeting, Reno, Nevada, January 1988.

16. Abstract
The statistical characteristics of wind-shear turbulence are modelled. Isotropic turbulence serves as the basis of comparison for the anisotropic turbulence which exists in a wind shear. The question of how turbulence "scales" in a wind shear is addressed from the perspective of power spectral density.

17. Key Words (Suggested by Author(s))	18. Distribution Statement
Anisotropic wind shear turbulence	Unclassified - Unlimited Subject Category 34

19. Security Classif. (of this report)	20. Security Classif. (of this page)	21. No. of pages	22. Price
Unclassified	Unclassified	32	A03

For sale by the National Technical Information Service, Springfield, Virginia 22161-2171

NASA-Langley, 1989